ACI STRUCTURAL JOURNAL TECHNICAL PAPER

Title no. 89-S52

Punching Shear Resistance of Flat Slabs: Influence of Reinforcement Type and Ratio

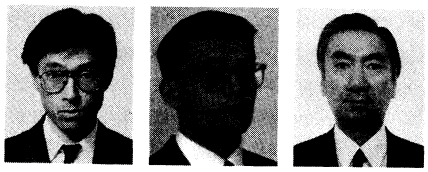

by Tetsuya Yamada, Antonio Nanni, and Katsushiko Endo

As a part of a research program to study the performance and design of flat-slab systems, this investigation aimed to determine the effect of shear reinforcement type and ratio on punching shear strength of monolithic slab-to-column connections. The first type of shear reinforcement consisted of hat-shaped units, very advantageous from the points of view of prefabrication and field installation. The second type consisted of double-hooked shear bars, more difficult to install but with very efficient anchorage. A total of 13 specimens were fabricated and tested. The dimensions of the slab were 2 x 2 x 0.2 m (79 x 79 x 7.9 in.), with a centrally located column 0.3 x 0.3 m (11.8 x 11.8 in.) in cross section. The column extended above and below the slab for a length of 0.3 m (11.8 in.). Monotonic static load was applied downwards at eight points symmetrically distributed around the column center at a distance of 0.75 m (29.5 in.). The specimen was supported by the column stud. Shear reinforcement varied from 0 to 1.53 percent in the first series, and from 0 to 1.98 percent in the second series. Longitudinal bars were placed on both compression and tension sides. The tensile flexural reinforcement was 1.23 and 1.53 percent in the first and second series, respectively. Load, deflection, and strain were monitored (at various locations along the shear and flexural reinforcement) during the tests. Experimental results showed that the hat-shaped shear reinforcement was not effective because of lack of proper anchorage and large spacing. Double-hooked reinforcement showed high effectiveness, which resulted in a considerable increment of the punching shear resistance of the connection. Comparisons with the provisions of ACI 318-89 were made.

Keywords: anchorage; bond (concrete to reinforcement); building codes; **flat concrete slabs; punching shear;** reinforced concrete; reinforcement spacing; shear properties; slab-column connections; structural design; tests.

In addition to limiting deflection under service loads, the greatest practical problem of flat-slab systems is punching shear failure at the slab-column connection region (ASCE-ACI 426 1974). When a shear capital or a drop panel is not used, it is rather difficult to assign the entire shear resistance to concrete alone and, at the same time, to maintain a limited slab depth. In recognition of this problem, the ACI Building Code Requirements for Reinforced Concrete (ACI 318-89, Section 11.12.3) permit the use of shear reinforcement, which can provide shear resistance V_s up to twice the value offered by concrete V_c. Shear resistance due to combined concrete and reinforcement V_n is limited to 1.5 times the value permitted for concrete when no reinforcement is used. These limitations are rather severe when compared to the case of beams. However, punching shear resistance of flat-slab systems is addressed even more restrictively in other building codes, such as the one presently enforced in Japan (Architectural Institute of Japan 1988), which does not allow consideration of any contribution of shear reinforcement.

ACI 318-89 recognizes that the effectiveness of shear reinforcement depends on its anchorage, even though it may be difficult to achieve in thin and medium-thickness slabs. For example, for slabs less than 22 cm (8.7 in.), either closed stirrups (enclosing a longitudinal bar at each corner) or vertical bars (with end anchorage capable of developing the yield strength of bars) can be used. The importance of shear reinforcement anchorage has been confirmed experimentally in a other studies (Lovrovich and McLean 1990; Broms 1990).

In the past, several papers have addressed the punching shear resistance of flat-slabs without shear reinforcement (Elstner and Hognestad 1956; Vanderbilt 1972; ASCE-ACI 426 1974; Regan 1984). These papers discuss the effect of concrete strength, flexural reinforcement, shear span, and test method. More recently, studies have been conducted to verify the effect of shear reinforcement (Seible and Ghali 1980; Lovrovich and McLean 1990; Broms 1990; Mortin and Ghali 1991) as lighter and more ductile construction becomes preferable. Different types of reinforcement, such as welded-wire fabric, studs, bent bars, and hooked bars were investigated. It was shown that shear reinforcement can improve both punching shear resistance and ductility. However, more experimental work is needed to study the effect of reinforcement quantity and to de-

ACI Structural, V. 88, No. 4, September-October 1992.
Received Sept. 23, 1991, and reviewed under Institute publication policies.

Tetsuya Yamada is a research engineer at the Technical Research Institute, Mitsui Construction Co., Japan. He has been involved in many projects concerned with building structures made of reinforced concrete, steel, and mixed members. His main research and design interests are in reinforced and prestressed concrete flat slab systems.

ACI member *Antonio Nanni* is an associate professor in the Department of Architectural Engineering at Pennsylvania State University. He received his PhD from the University of Miami in 1985. His research interests are in concrete materials and structures. He is Chairman of ACI Committee 440, FRP Reinforcement, and is a member of Committees 325, Concrete Pavements; 544, Fiber Reinforced Concrete; and 549, Ferrocement and Other Thin Reinforced Products.

Katsushiko Endo is a chief research engineer at the Research and Development Department, Mitsui Construction Co., Japan.. He has been involved in many research and development projects on concrete structures. His current research interests are mixed structures with steel and reinforced concrete members.

velop more realistic testing methods and easier-to-construct/install shear reinforcement. Finally, research on the behavior of flat slabs is particularly important in Japan, where experimental and practical experience with this construction system is still limited.

This paper reports the results of an experimental and analytical study on punching shear, during which 13 monolithic slab-to-column connections were tested. The test variables of the study included two types of shear reinforcement used at five and six different percentages, respectively. The major difference between the two reinforcement types was anchorage and ease of installation.

The first type of shear reinforcement (termed hat-type) consisted of a prefabricated cage (unit) made of hat-shaped bars welded to two horizontal straight bars. Units were placed side by side during assembly of the specimen reinforcement. To maximize ease of prefabrication of the units as well as installation, no provision was made to enclose longitudinal bars at the corners of the hat-shaped bar. For this reason, and because hat-type bars are open-shaped, this reinforcement type did not conform with the requirements of ACI 318-89.

The second type of shear reinforcement (termed hook-type) consisted of individual bars with a 180-deg hook at each end. The hooks were bent on orthogonal planes so that one bar could be anchored to top and bottom longitudinal reinforcing bars in the two orthogonal directions. One of the potential advantages of this configuration is that shear reinforcement can be contained between longitudinal reinforcing bars without requiring additional concrete cover. The objective of the experimental investigation was to determine the effects of the two shear reinforcement types and the interaction between shear and moment at different shear reinforcement ratios.

RESEARCH SIGNIFICANCE

The tests described in this paper show that properly anchored and spaced shear reinforcement increases punching shear resistance and ductility of flat-slab to column connections. The safety factor between observed punching shear strength and values predicted according to ACI 318-89 is appropriate for low reinforcement ratios, but may be too conservative at high ratios.

EXPERIMENTAL PROGRAM

Materials

Concrete was specified to have a minimum 28-day compressive strength of 21 MPa (3046 psi). Deformed steel bars were used for all types of reinforcement. Three steel grades were used: SD80 and SD50 [f_y = 800 and 500 MPa (116,026 and 72,516 psi)] for the longitudinal bars, and SD30 (f_y = 300 MPa = 43,510 psi) for the shear reinforcement. Bar size varied between 6 and 16 mm (0.2 and 0.6 in.) in diameter (D6 to D16).

Specimens

The elevation of the typical slab-to-column connection specimen is shown in Fig. 1(a). The dimensions of the slab were 2 by 2 by 0.2 m (79 by 79 by 7.9 in.), with a centrally located column 0.3 by 0.3 m (11.8 by 11.8 in.) in cross section. The column extended above and below the slab for a length of 0.3 m (11.8 in.). The specimen was supported by the lower column-stud resting directly on the laboratory floor.

Table 1 shows the slab reinforcement characteristics of each sample. The first series (Codes T1 to T6) consists of six specimens using hat-type shear reinforcement. The second series (Codes K1 to K7) is relative to the seven samples with hook-type shear reinforcement. Column 2 in Table 1 summarizes the characteristics of the longitudinal reinforcement which is also schematically presented in Fig. 1(b) and 1(c). For both series, longitudinal reinforcement was symmetrically distributed in the orthogonal X and Y directions with minimum clear cover of 20 mm (0.8 in.) at both top and bottom slab faces. For all specimens and for both top and bottom faces, bars in the X direction were placed directly above bars in the Y direction. This flexural reinforcement arrangement provides identical clearance in the two orthogonal directions if two-way prestressing cables are used. In the T-series, 13-mm (0.5-in.) diameter bars were spaced at 60 mm (2.4 in.) in the tensile (top) zone (reinforcement ratio P_t = 1.23 percent) and at 120 mm (4.7 in.) in the compressive (bottom) zone (reinforcement ratio P_c = 0.62 percent). For the K-series, 16-mm (0.6-in.) diameter bars spaced at 80 mm (3.1 in.) were used in both tensile and compressive zone (P_t = P_c = 1.53 percent). The column reinforcement consisted of four D16 corner bars and D10 ties spaced at 50 mm (2.0 in.) in all specimens.

Shear reinforcement characteristics are given in Columns 4 to 8 of Table 1. For the T-series, the shear reinforcement ratio was varied from 0 to 1.53 percent (Column 6) by changing the hat-bar diameter (Column 4) and/or hat-bar spacing in each unit (Column 8). A typical prefabricated unit of the hat-type shear reinforcement is shown in Fig. 2. The hat-bar width and the spacing between adjacent units was maintained constant for all specimens and equal to 100 mm (3.9 in.). Hat-bar spacing a and hat-bar diameter d were varied

in each specimen as described in Table 1. For each hat-type unit, the development length (rim of the hat) was equal to eight diameters and such that it would fit under longitudinal bars in the perpendicular direction. As shown in Fig. 3, the unit positioned at the center of the slab and intersecting the column had the first hat-bar starting at the column interface.

For the K-series, the shear reinforcement ratio was varied from 0 to 1.98 percent (Column 6 of Table 1) by changing bar diameter (Column 4) and/or bar spacing (Column 8). Two different spacings were obtained by placing a bar at every node of the longitudinal reinforcement grid (interval equal to 1) or at every second node (interval equal to 2) as shown in the sketch of Fig. 4(a). The typical hook-type bar is shown in Fig. 4(b). The sketch shows that the length of the bar h had to be changed according to the corresponding diameter. The extension of the 180-deg hook was in all cases six times the bar diameter. The sketch also shows the twisted hooks to allow for anchorage on mutually perpendicular longitudinal bars. Fig. 5 shows the arrangement of D6 hook-bars at every second node (Specimen K2).

Loading and instrumentation

Monotonic static load was applied downwards at eight points symmetrically distributed around the column center at a distance of 0.75 m (29.5 in.). The lower column stud acted as the reaction support [Fig. 1(a) to (c)]. The load was applied by two hydraulic jacks connected to the same pump, and set in deflection-control. Fig. 6 shows a specimen under test.

Measurements included: load delivered by the two jacks, vertical deflection taken from the bottom side of the slab at a distance of 50 mm (2.0 in.) from the column face, and strain in shear and flexural reinforcing bars at various locations. The function of the numerous strain gages was to provide information on internal force distribution in the reinforcement and occurrence of yielding. Crack formation on the concrete slab top-surface was monitored during testing. At the conclusion of tests, a quarter of the slab of each specimen was sawn off to inspect crack propagation through the depth of the slab.

TEST RESULTS

Load deflection

Fig. 7(a) and (b) show the load-deflection curves for the T-series and K-series, respectively. Given the position of deflection measurement, it is assumed that the recorded deflection is primarily caused by shear deformation, rather than flexure deformation. With reference to Fig. 7(a), it is seen that the inclusion of hat-type shear reinforcement improves peak-load as compared to the case with no shear reinforcement (T1). However, with the exception of Specimen T2, all other shear-reinforced specimens have approximately the same peak load. Vertical deflection at peak load for the shear-reinforced specimens is between 1.5 and 1.7 times that of Specimen T1. In terms of post-peak behavior, the load-carrying capacity of Specimen T1 is halved at a deflection of approximately 6 mm (0.2 in.), whereas none of the other specimens show significant loss of strength over the same deflection interval.

With reference to Fig. 7(b) (hook-type reinforcement), the increment in peak-load of reinforced versus

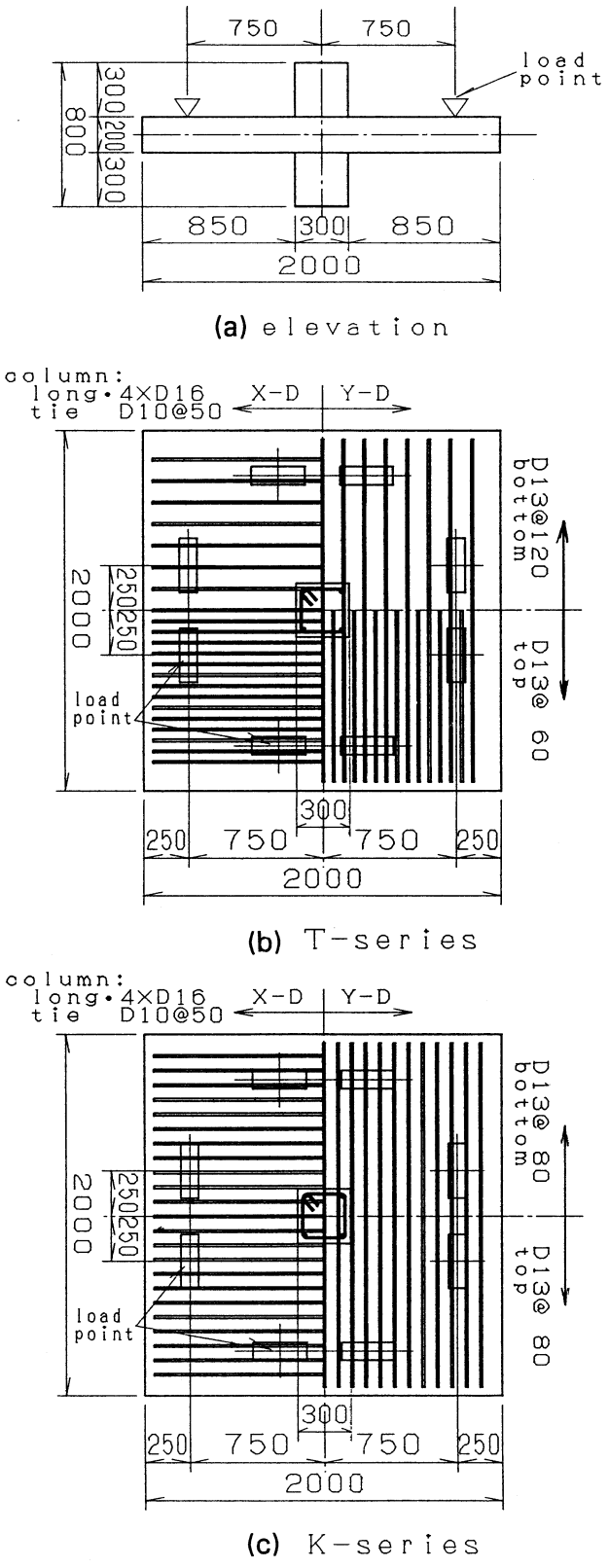

Fig. 1—Specimen geometry and arrangement of longitudinal reinforcement (dimensions in mm; 1 mm = 0.039 in.)

unreinforced specimens is higher than in the case of the T-series. Furthermore, deflection at peak-load of Specimens K2 to K7 is approximately five times larger than that of Specimen K1. For most of the reinforced specimens, peak-load is reached after considerable plastic deformation. Also, the strength degradation after peak-load for shear-reinforced specimens is very small.

Cracking and failure pattern

In every specimen, flexural cracks occurred first. They radially advanced from the column faces towards the slab edges along the four axes of symmetry of the slab (central X and Y axes and two diagonals). Subsequently, circular concentric cracks developed around the column. Different failure patterns were observed in different specimens. Fig. 8 shows the sawn-off sections of three representative specimens, T4, K4, and K7.

For Specimen T4 [Fig. 8(a)], extensive cracking parallel to the longitudinal tensile reinforcing bars developed from the end of the inclined shear crack starting at the column face. (A similar split-crack pattern is found along the longitudinal reinforcement of beams without stirrups as a result of dowel action.) The inclined shear crack from the column face had a slope greater than 45 deg and did not intersect any hat-bar, since hat-bar spacing in this case was more than $d/2$ (d = longitudinal reinforcement average depth). For this reason, the peak-load of Specimen T4 was smaller than that of Specimen T3, which had a smaller reinforcement ratio but also a smaller spacing. In Specimen T4, the cracked region extended through the compressive zone of the joint. At ultimate failure, the specimen divided into two parts along the horizontal split crack at the top and the inclined crack starting at the column face.

For Specimen K4 [Fig. 8(b)], extensive inclined shear cracks can be observed in the connection zone immediately adjacent to the column face. These cracks surfaced at the top side of the slab at a distance of approximately $1.5d$ from the column face. A number of hook-type bars were intersected by each inclined crack. For this specimen (as well as the rest of reinforced K-series specimens), split-cracking along the longitudinal reinforcement, as found in Sample T4, did not occur.

In Specimen K7 [Fig. 8(c)], the collapse circle line was only at $0.5d$ from the column face. The direction of penetration into the slab of this crack is practically vertical, to indicate that it was flexure-induced. Some shear cracks with a slope of 45 deg also developed, but did not surface. Cracks at ultimate failure were still very tight and small in number. Crushing of concrete in the compression zone of the connection (not the joint) was responsible for ultimate failure.

Strain distribution

Fig. 9 shows strain distribution in the shear reinforcement of the same specimens (T4, K4, and K7) discussed in the previous section. Strain is shown at practically identical levels of load for all specimens. In the case of Specimen T4, even at peak-load, the strain level was very small (less than 200 microstrains), indicating that the shear reinforcement was ineffective. On the contrary, the hook-bars of Specimen K4 placed at distance $d/2$ and d from the column face, reached the yielding point at approximately 80 percent of peak-load. As shown in Fig. 9(b), these bars intersected inclined shear cracks and were, therefore, very effective in resisting shear forces. In the case of Specimen K7 [Fig. 9(c)], even though the levels of applied load were considerably higher than that of Specimen K4, strain in the shear reinforcement was below 1000 microstrain. This is because ultimate failure was flexure-controlled and inclined shear cracks did not develop. For each of the specimens given in Fig. 9, the tensile strain in the flexural reinforcement is also shown at ultimate load. Longitudinal reinforcing bars yielded in the case of Specimens K4 and K7.

Table 1 — Specimen reinforcement characteristics

Specimen code	Flexural reinforcement	Shear reinforcement					
		Shape	Size	Grade	P_w, percent	Development length	Arrangement a, cm
(1)	(2)	(3)	(4)	(5)	(6)	(7)	(8)
T1	Size = D13 Grade = SD80 P_t = 1.23 percent at 60 mm P_c = 0.62 percent at 120 mm	Hat-type	—	—	0.00	—	—
T2			D10	SD30	0.51	8d	14.0
T3			D10		0.75		9.5
T4			D13		0.97		13.0
T5			D13		1.27		10.0
T6			D16		1.53		13.0
K1	Size = D16 Grade = SD50 P_t = 1.53 percent at 80 mm P_c = 1.53 percent at 80 mm	Hook-type	—	—	0.00	—	Interval
K2			D6	SD30	0.25	6d	2
K3			D6		0.50		1
K4			D10		0.55		2
K5			D10		1.11		1
K6			D13		0.99		2
K7			D13		1.98		1

P_t = Top reinforcement ratio; P_c = bottom reinforcement ratio; P_w = Shear reinforcement ratio; a = hat-bar spacing; d = Bar diameter.

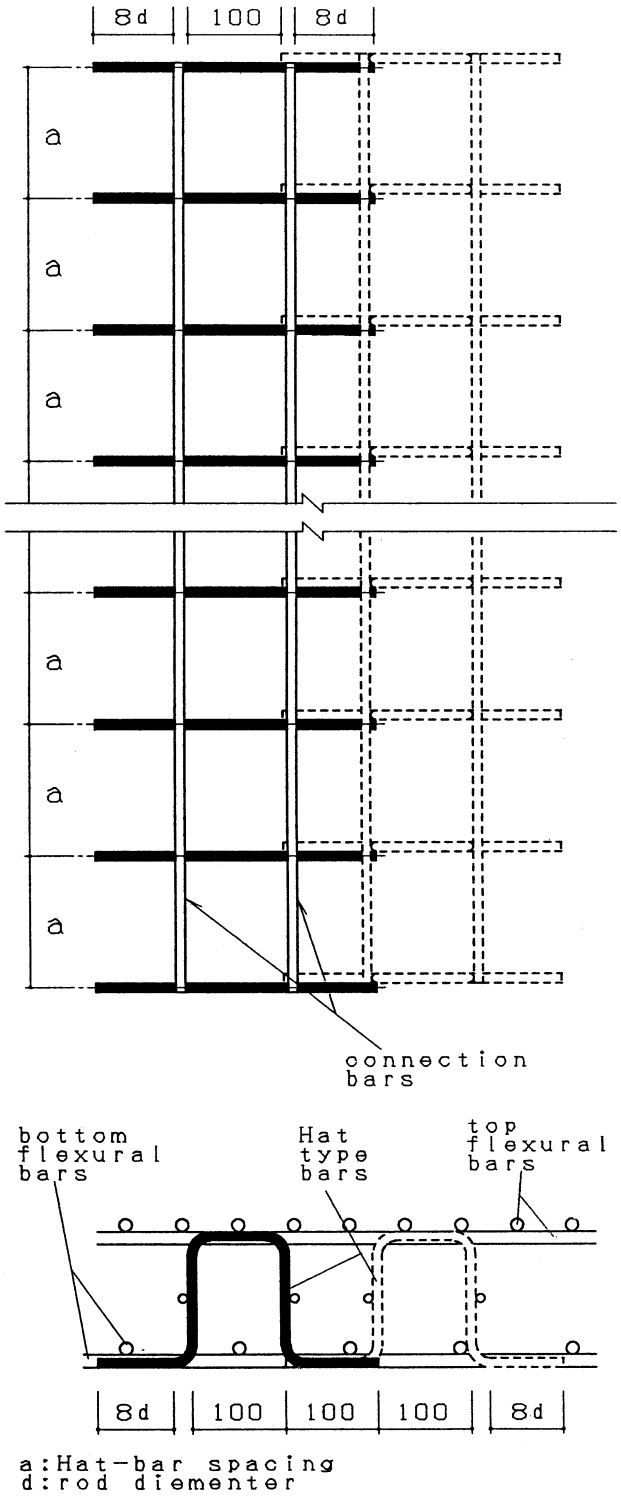

Fig. 2— Hat-type shear reinforcement; a = *hat-bar spacing;* d = *bar diameter (dimensions in mm; 1 mm = 0.039 in.)*

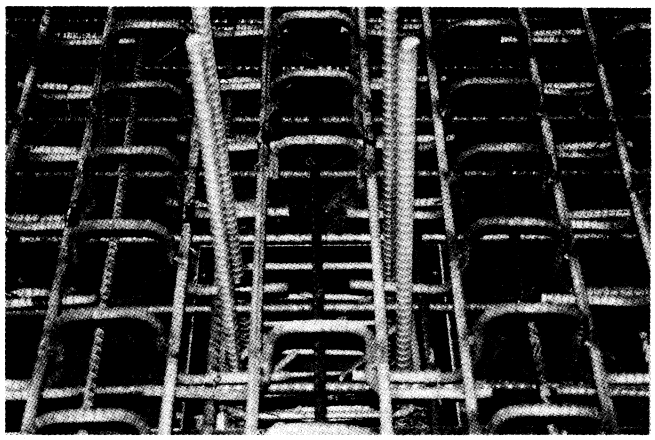

Fig. 3—Position of hat-type reinforcement with respect to column

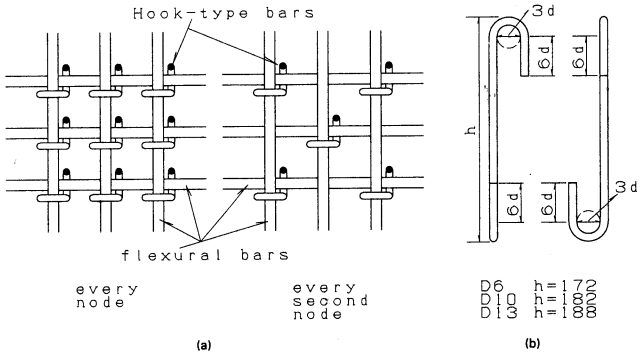

Fig. 4—Hook-type shear reinforcement (dimensions in mm; 1 mm = 0.039 in.)

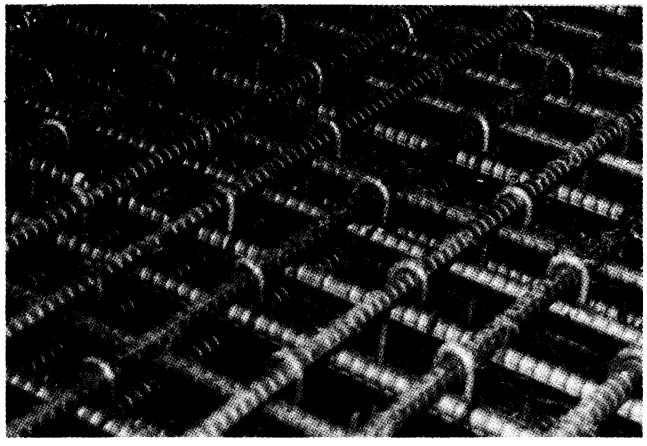

Fig. 5—Arrangement of hook-type reinforcement

For other specimens of the K-series, namely K2 and K3, shear reinforcement also yielded prior to ultimate failure. In these two specimens, since a reinforcement ratio smaller than in the case of K4 was provided, the number of yielded hook-bars was higher and the yield zone approached the loading points. On the contrary, Specimens K5 and K6 behaved very similarly to K7: shear reinforcement did not yield and flexural reinforcing bars yielded in the proximity of the column face. For these two samples, ultimate failure was flexure-controlled.

DISCUSSION

Shear stress versus shear reinforcement

Fig. 10 shows the relationship between shear stress in

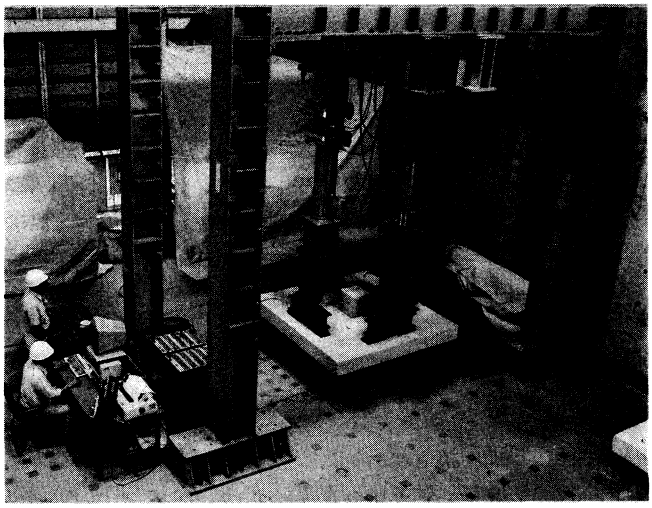

Fig. 6—Specimen under test

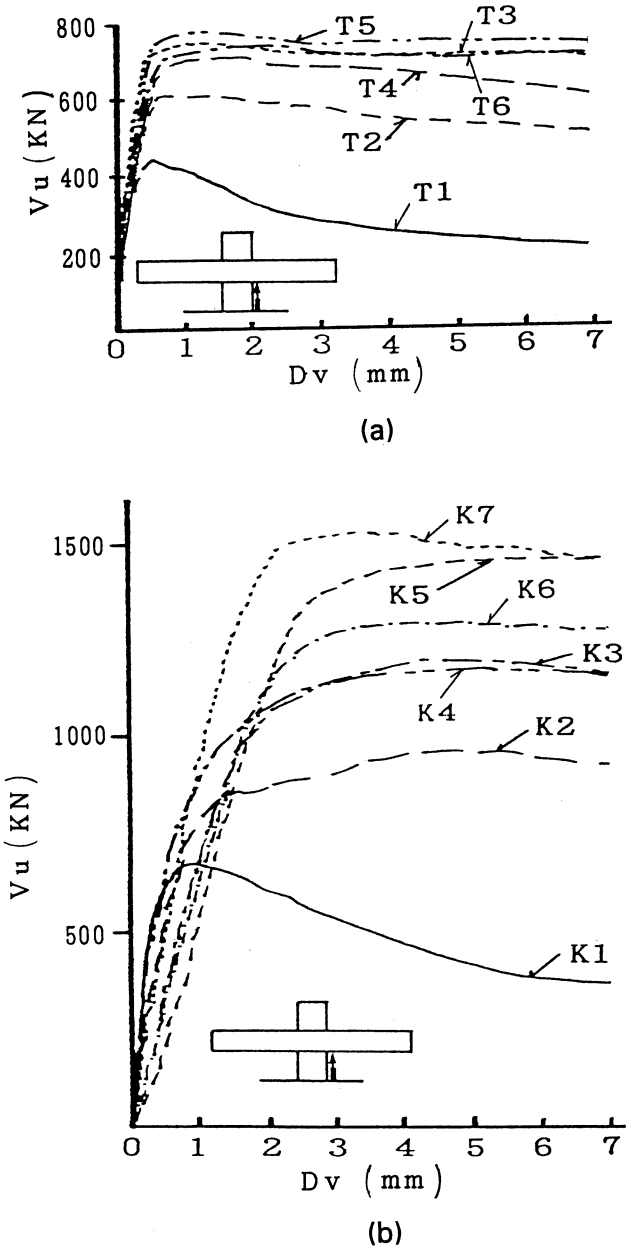

Fig. 7— Load-deflection curves for T-series and K-series (1 mm = 0.039 in; 1 kN = 225 lb)

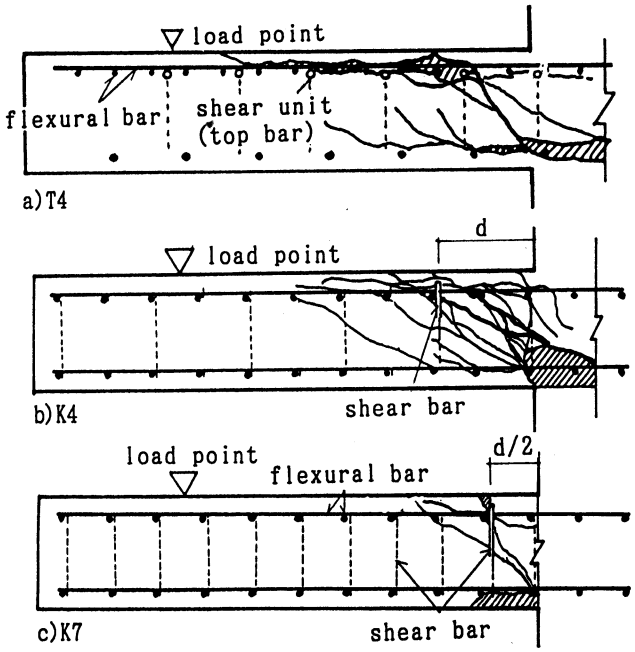

Fig. 8— Crack pattern through slab depth

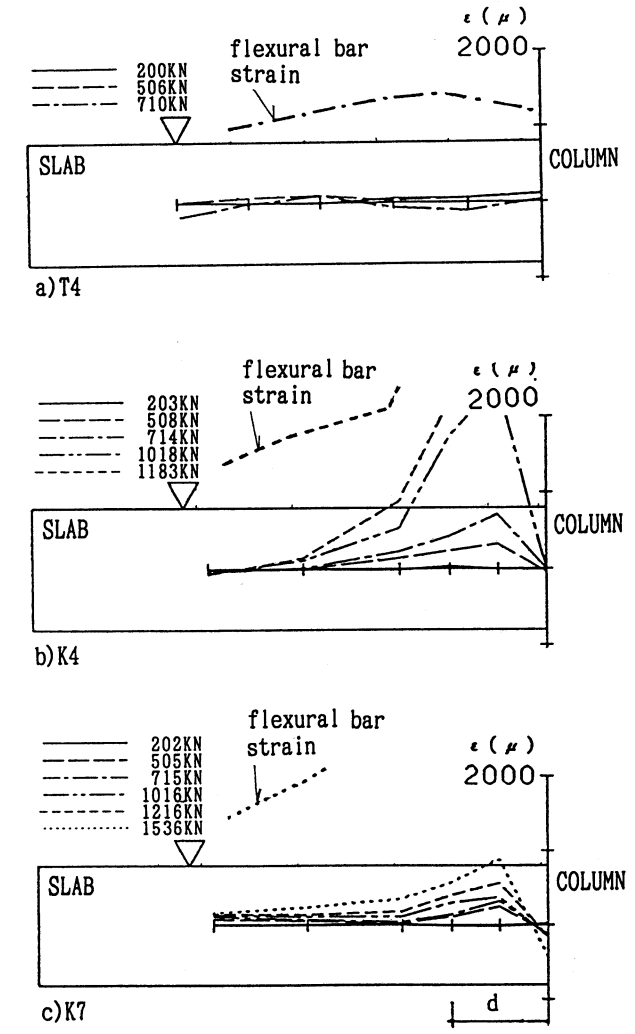

Fig. 9—Strain distribution in shear and flexural (tensile) reinforcement (1 kN = 225 lb)

concrete and reinforcement ratio. Shear stress at peak load was computed as an average value at a distance $d/2$ from the column face. In this figure, the circle symbols are relative to the T-series, and the cross symbols are relative to the K-series. All data points represent shear-controlled failures unless included in brackets, in which case they indicate flexure-controlled failures. The difference in shear resistance between the two unreinforced Specimens T1 and K1 (after accounting for concrete strength variation) is due to a difference in longitudinal reinforcement percentage (P_t and P_c in Specimen K1 are larger than the corresponding percentages in Specimen T1, particularly in the compressive zone).

For the T-series, the specimen with 0.5 percent reinforcement ratio (T2) shows an increment in maximum shear stress of approximately 35 percent with respect to the unreinforced sample (T1). For higher values of the shear reinforcement ratio (0.7 to 1.5 percent), further increase in maximum stress levels off at approximately 65 percent. Due to lack of proper anchorage and wide spacing between hat-bars, the presence of shear reinforcement was not very effective in improving punching shear resistance.

For the K-series, when the reinforcement ratio is about 0.5 percent (K3 and K4), the increment in maximum shear stress with respect to the unreinforced sample (K1) is approximately 80 percent (significantly better than the corresponding sample in the T-series because of smaller spacing and proper anchorage). For reinforcement ratios of 1.0 percent and larger, no appreciable increase in maximum stress over a threshold of approximately 120 percent was obtained because the specimens failed in flexure.

Comparison with ACI 318-89

Table 2 shows a comparison between the experimental results and predicted values according to ACI 318-89. Shear resistance was computed in two ways: first, by considering only the contribution of concrete ($V_{n,1}$), and, second, by including the contribution of shear reinforcement ($V_{n,2}$), irrespective of its compliance with reinforcement anchorage and spacing requirements in the code. Column 6 in Table 2 shows the shear resis-

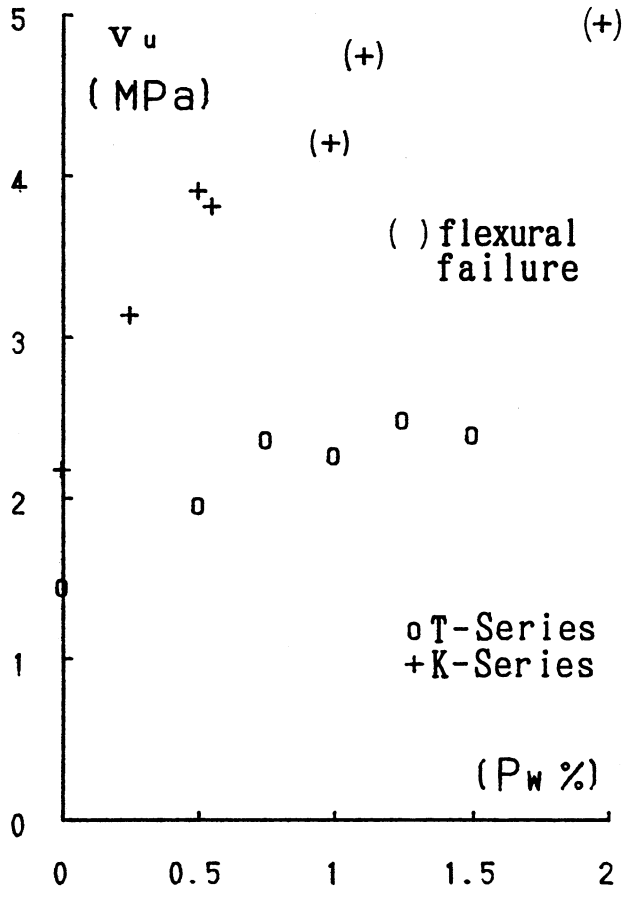

Fig. 10—Concrete shear stress versus reinforcement ratio (1.0 MPa = 145 psi)

Table 2 — Experimental versus ACI 318-89 values

Code	f_c, MPa	f_{yf}, MPa	f_{yv}, MPa	V_u, kN	ACI Building Code					
					$V_{c1} = V_{n1}$, kN	V_{c2}, kN	V_s, kN	V_{n2}, kN	V_u/V_{n1}	V_u/V_{n2}
(1)	(2)	(3)	(4)	(5)	(6)	(7)	(8)	(9)	(10)	(11)
T1	21.58	811		441	477	239	0	477	0.92	0.92
T2	23.35		361	600	496	248	570	745	1.21	0.81
T3	23.74		361	727	501	250	838	751	1.45	0.97
T4	24.43		331	697	508	254	993	762	1.37	0.91
T5	22.66		331	762	489	245	1299	734	1.56	1.04
T6	24.33		367	735	507	253	1737	760	1.45	0.97
K1	26.00	568		658	507	262	0	507	1.30	1.30
K2	27.17		347	950	518	268	264	532	1.83	1.79
K3	25.90		347	1183	506	261	528	759	2.34	1.56
K4	27.37		317	1153	520	269	531	780	2.22	1.48
K5	26.00		317	1440	507	262	1072	760	2.84	1.89
K6	26.39		330	1274	511	264	992	766	2.50	1.66
K7	27.76		330	1498	524	271	1985	786	2.86	1.91

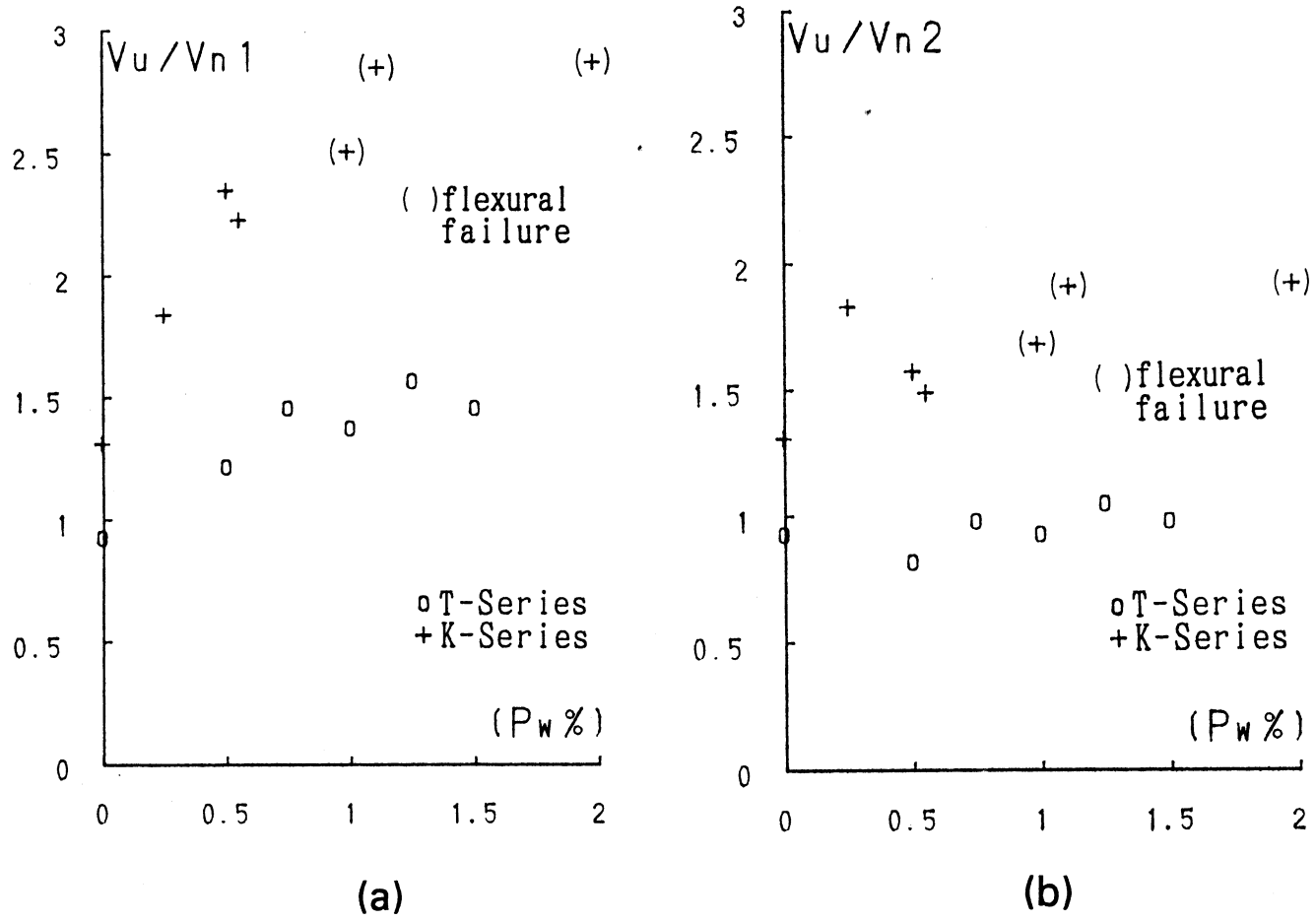

Fig. 11—Experimental-to-computed shear strength ratio versus reinforcement ratio

tance $V_{n,1}$ according to ACI 318-89 Eq. (11-38) ($4 \cdot 0.083\sqrt{f'_c} \cdot b_o \cdot d$ in N). The ratio of maximum load to shear capacity ($V_u/V_{n,1}$) is given in Column 10 and plotted as a function of the reinforcement ratio in Fig. 11(a). Column 9 in Table 2 shows the shear resistance $V_{n,2}$ according to Eq. (11-2), with the limitations specified in 11.12.3 ($V_c = 2 \cdot 0.083\sqrt{f'_c} \cdot b_o \cdot d$, and $V_n \leqslant 6 \cdot 0.083\sqrt{f'_c} \cdot b_o \cdot d$, in N). The ratio maximum load to shear capacity ($V_u/V_{n,2}$) is given in Column 11 and plotted as a function of the reinforcement ratio in Fig. 11(b).

By considering Fig. 11(a) and (b), it appears that the two series have clearly distinct performances. The T-series shows that when shear resistance is computed using concrete only [Fig. 11(a)], there is a very modest improvement in experimental-to-computed strength ratio as a function of shear reinforcement percentage. The presence of shear reinforcement is not detrimental to strength but hardly justifiable. Fig. 11(b), where all data points for the T-series but one fall below the strength ratio value of 1.0, shows that hat-type reinforcement (without longitudinal bars enclosed at the corners and with a spacing larger than $d/2$) cannot be considered as a component of the shear strength equation irrespective of the reinforcement percentage (as prescribed by ACI 318-89).

For the K-series, Fig. 11(a) shows that computed shear strength based only on concrete would widely underestimate experimental values. Properly spaced and anchored shear reinforcement increases punching shear resistance. When the computed strength includes the reinforcement contribution [Fig. 11(b)], the equation proposed in ACI 318-89 is justifiably conservative for reinforcement ratios up to 0.6 percent. For higher values of the reinforcement ratio, the real experimental-to-computed shear strength ratios would be higher if flexural-type failures had not occurred.

Moment-shear interaction

In the K-series, two types of collapse were observed. The first type is a shear-controlled failure (K1, K2, K3, and K4) and second type is a flexure-controlled failure (K5, K6, and K7). Fig. 12 shows the relationship between ultimate moment and ultimate shear for this series. The horizontal axis represents the ratio V_u/V_n, where V_n is computed as shown in Eq. (1) (no upper limitation), assuming a rectangular failure line at $d/2$ from the column faces. The vertical axis represents the ratio M_u/M_n, where M_n is computed as shown in Eq. (2) for four strips having an effective width of 90 cm (35.4 in.) (column width plus three times the slab depth = $c + 3 \cdot h$). In the case of moment, the critical section coincides with the column face

$$V_n = 4 \cdot 0.083 \sqrt{f'_c} \cdot b_o \cdot d + P_w \cdot b_o \cdot d \cdot f_{y,v} \quad \text{(in N)} \quad (1)$$

$$M_n = 4 \cdot 0.9 \cdot P_t \cdot (c + 3 \cdot h) \cdot d \cdot f_{y,f} \quad \text{(in N)} \quad (2)$$

Experimental data points are fitted with a regression curve which is assumed to have the equation of a circle. Using the Levenberg-Marquardt regression formula, the following expression is found

$$X^2 + Y^2 = 1.43^2 \quad (3)$$

where $X = V_u/V_n$; $Y = M_u/M_n$; and the residual sum of squares = 0.038.

According to Fig. 12 (amount of flexural reinforcement constant for all samples), data points above the diagonal (Y = X) line represent flexure-controlled failures and data points below this line represent shear-controlled failures. The intersection point between the diagonal line and the regression circle has coordinates practically equal to one ($V_u/V_n = 1$; $M_u/M_n = 1$). This means that the proposed method for computing V_n and M_n can predict simultaneous failure. For practical purposes, since slab failures need to be flexure-controlled, the shear ratio V_u/V_n has to be less than one.

CONCLUSIONS

Based on the results obtained in this research, the following conclusions may be drawn:

1. The significant differences between hat-type (T-series) and hook-type (K-series) shear reinforcement is the result of anchorage and spacing. Anchorage to longitudinal top and bottom bars is necessary and bar spacing should be less than $d/2$. Lack of good anchorage in the hat-type reinforcement was not due to insufficient development length but resulted from the lack of longitudinal corner bars. Bar spacing less than $d/2$ is needed to intercept inclined cracks. In the K-series, this was accomplished even when hook-bars were placed every second longitudinal-bar node (spacing equal to d) because of staggering.

2. Specimens K3 and K4 have the same shear reinforcement ratio obtained with small diameter bars at every node and with large diameter bars at every second node, respectively. Comparing the load-deflection curves for these two specimens, the same punching shear resistance and ductility is observed.

3. The presence of shear reinforcement, even if not effective in increasing punching shear resistance as for the case of the T-series, affected the shape of the load deflection curve in the post-peak region by inhibiting strength degradation.

4. ACI 318-89 provisions for the computation of shear strength considering the reinforcement contribution are justifiably conservative at low reinforcement ratios (up to approximately 0.6 percent). For larger values of the reinforcement ratio, the $6.0 \cdot 0.83\sqrt{f'_c} \cdot b_o \cdot d$ (in N) limitation may be excessively conservative.

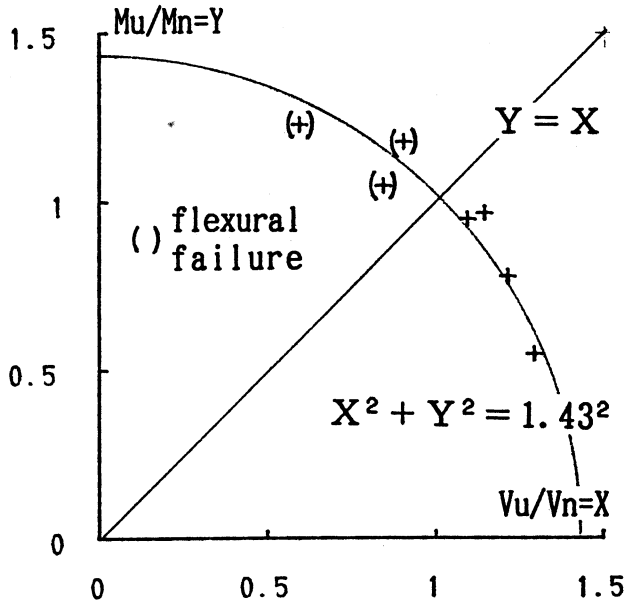

Fig. 12—Shear-moment interaction diagram

5. Experimental results relative to effective shear reinforcement (K-series) can be represented by the regression formula $(V_u/V_n)^2 + (M_u/M_n)^2 = 1.43^2$, when nominal shear and moment resistance is computed as proposed. Further research should establish if this relationship is maintained for different amounts of flexural reinforcement.

REFERENCES

ACI Committee 318, 1990, "Building Code Requirements for Reinforced Concrete and Commentary," (ACI 318-89 and ACI 318R-89), American Concrete Institute, Detroit, 353 pp.

ASCE-ACI Joint Committee 426, 1974, "Shear Strength of Reinforced Concrete Members—Slabs," *Journal of the Structural Division,* ASCE, V. 100, No. 8, pp. 1543-1559.

Architectural Institute of Japan, 1988, "Standard for Structural Calculation of Reinforced Concrete Structures," Tokyo, pp. 106-109. (in Japanese)

Broms, Carl Erik, 1990, "Shear Reinforcement for Deflection Ductility of Flat Plates," *ACI Structural Journal,* V. 87, No. 6, Nov.-Dec., pp. 696-705.

Elstner, Richard C., and Hognestad, Eivind, 1956, "Shearing Strength of Reinforced Concrete Slabs," ACI JOURNAL, *Proceedings* V. 53, No. 7, July, pp. 29-58.

Lovrovich, John S., and McLean, David I., 1990, "Punching Shear Behavior of Slabs with Varying Span-Depth Ratios," *ACI Structural Journal,* V. 87, No. 5, Sept.-Oct., pp. 507-511.

Mortin, John D., and Ghali, Amin, 1991, "Connection of Flat Plates to Edge Columns," *ACI Structural Journal,* V. 88, No. 2, Mar.-Apr., pp. 191-198.

Regan, P. E., 1984, "Dependance of Punching Resistance upon the Geometry of the Failure Surface," *Magazine of Concrete Research,* V. 36, No. 126, Mar., pp. 3-8.

Seible, Frieder; Ghali, Amin; and Dilger, Walter H., 1980, "Preassembled Reinforcing Units for Flat Plates," ACI JOURNAL, *Proceedings* V. 77, No. 1, Jan.-Feb., pp. 28-35.

Vanderbilt, M. D., 1972, "Shear Strength of Continuous Plates," *Journal of the Structural Division,* ASCE, V. 98, No. 5, May, pp. 961-973.